Journal of Electroanalytical Chemistry 706 (2013) 48–54

Contents lists available at ScienceDirect

Journal of Electroanalytical Chemistry

journal homepage: www.elsevier.com/locate/jelechem

Correlation between pore size and reactivity of macro/mesoporous iron and copper hexacyanoferrates for H_2O_2 electrocatalysis

Vinicius R. Gonçales [a], Martin H. Gaitán [b], Alann de O.P. Bragatto [a], Galo J.A.A. Soler-Illia [c], Luis M. Baraldo [b], Susana I. Córdoba de Torresi [a,*]

[a] Instituto de Química, Universidade de São Paulo, POBox: 26077, Butantã, São Paulo, SP, Brazil
[b] INQUIMAE, Facultad de Ciencias Exactas y Naturales, Universidad de Buenos Aires, Pabellón 2, Ciudad Universitaria, C1428EHA Buenos Aires, Argentina
[c] Gerencia de Química, Comisión Nacional de Energia Atómica, Centro Atómico Contituyentes, San Martín, B1650KNA Buenos Aires, Argentina

ARTICLE INFO

Article history:
Received 12 June 2013
Received in revised form 23 July 2013
Accepted 24 July 2013
Available online 14 August 2013

Keywords:
Porous
Hydrogen peroxide
Prussian blue
Polypyrrole
Copper hexacyanoferrate
Template

ABSTRACT

The effect of pore size to H_2O_2 detection by macroporous and mesoporous Prussian blue type electrocatalysts is reported in the present paper. The macroporous electrocatalysts were prepared employing spherical colloidal particles of different sizes (300, 460, 600 and 800 nm) as sacrificial templates to synthesize a copper hexacyanoferrate/polypyrrole (CuHCNFe/Ppy) hybrid material. Surprisingly, macroporous and non-porous CuHCNFe/Ppy displayed very similar results, which led to a discussion that application of macroporous platforms in sensors must consider the material wettability and the influence of electrochemical kinetics on analyte detection. In order to evaluate the effect of smaller pores, the performance of the macroporous H_2O_2 sensors was also compared to electrocatalysts synthesised through the immobilization of Prussian blue and CuHCNFe layers inside the cavities of mesoporous TiO_2 films with diameters of 13, 20 and 40 nm. In this scale, the results were superior than those achieved with the non-porous sensors, demonstrating the possibility of controlling the performance of H_2O_2 sensors according to the pore diameter and the amount of immobilized material. Among the tested porous materials, the H_2O_2 sensor with better performance was achieved using the 20-nm diameter TiO_2 platform functionalized with Prussian blue, which presented a sensitivity of (930 ± 50) μA cm^{-2} mmol^{-1} L, detection limit of (0.49 ± 0.08) μmol L^{-1}, response time of (6 ± 2) seconds and linear range up to (1.3 ± 0.1) mmol L^{-1}. This performance was extremely satisfactory considering sensors operating by chronoamperometry.

1. Introduction

Close-packed arrays of monodisperse polystyrene or silica particles have been successful employed to develop electrochemical sensors and biosensors [1–7]. After removing the spherical particles, the resulting film is a true cast of the template structure. Following a similar methodology, surfactant micelles can also be used as templates instead of the colloidal particles. However, in this case, the resulting mesoporous structure presents dimensions comparable to the diameter of the used amphiphilic aggregates. Both strategies are interesting because they allow the formation of three-dimensional materials with high electroactive surface area/volume ratio, allowing good accessibility of the electrolyte to inner active sites and presenting electronic conductivity through the walls of the material up to the current collector [8–10].

For clinical electrochemical sensors, it is well known that direct H_2O_2 quantification can present significant signal interference. As a result, electrodes have been modified with metal-hexacyanoferrate-based electrocatalysts to produce high-selectivity H_2O_2 sensors capable of operating between −0.20 and 0.00 V (vs Ag/AgCl/KCl_{sat}) with fast and sensitive responses [11–14].

The present work utilizes close-packed arrays of spherical colloidal polystyrene particles and lyotropic liquid crystalline phases to produce macroporous and mesoporous metal-hexacyanoferrate-based sensors. In the first case, polystyrene spheres with diameters of 300, 460, 600 and 800 nm were used to synthesize a hybrid copper hexacyanoferrate/polypyrrole (CuHCNFe/Ppy) material. As described in previous works, the incorporation of a metal-hexacyanoferrate electrocatalyst into a conducting polymer could drastically improve the mechanical and electroanalytical properties of the resulting sensors [15,16]. Metal hexacyanoferrate-based sensors with pores at nanoscale were also produced

Abbreviations: CuHCNFe, copper hexacyanoferrate; CuHCNFe/Ppy, copper hexacyanoferrate/polypyrrole.

* Corresponding author. Tel.: +55 11 30919177; fax: +55 11 38155579.
E-mail address: strorresi@iq.usp.br (S.I. Córdoba de Torresi).

1572-6657/$ - see front matter © 2013 Elsevier B.V. All rights reserved.
http://dx.doi.org/10.1016/j.jelechem.2013.07.029

through the immobilization of the electrocatalyst into mesoporous TiO_2 platforms previously synthesised around surfactant micelles templates in hexagonal phase [17,18]. In this case, TiO_2 with pore diameters of 13, 20 and 40 nm were modified with CuHCNFe and Prussian blue films by coordination-assisted layer-by-layer deposition.

The objective of the paper is to study the importance of pore size to H_2O_2 detection by macroporous and mesoporous Prussian blue type electrocatalysts. The paper is focused on the employment of Prussian blue, since it is very active and selective for H_2O_2 reduction, and also on copper hexacyanoferrate (CuHCNFe), since it is active in the presence Na^+, which is a Prussian blue cation commonly found in biological samples. The comparison of both methodologies contributes to our understanding of the importance of pore size on H_2O_2 sensors performance, affecting both the wettability and reactivity of the electrocatalyst.

2. Methodology

2.1. Reagents

Polystyrene latex spheres with diameters of 300, 460, 600 and 800 nm were obtained from Aldrich as 10 wt% dispersions in water. All reagents were used as received except pyrrole, which was distilled prior to use. H_2O_2 was purchased from Sigma–Aldrich as a 30 wt% aqueous solution. Purified water (UHQ Elga System 18 MΩ cm) was used to prepare the solutions.

2.2. Instrumentation

Cyclic voltammetry and chronoamperometry experiments were performed with an Autolab PGSTAT 30 (Eco Chemie). All potentials were referred to an $Ag/AgCl/KCl_{sat}$ electrode, while a platinum foil was employed as the auxiliary electrode. The morphologic images were obtained from field emission scanning electron microscopy (FESEM, JSM-7401F from JEOL). The UV–Vis spectra were acquired on a HP8453 Hewlett–Packard spectrophotometer. Contact angle experiments were performed in a GBX Instrumentation Scientifique instrument coupled to a Nikon PixeLink camera.

2.3. Deposition of macroporous and non-porous CuHCNFe/Ppy on glassy carbon electrode

The CuHCNFe/Ppy synthesis was performed in two electrochemical steps. The methodology was based on previous publications [2,3], but here the number of voltammetric cycles was controlled as a function of the desired deposition charge.

Briefly, polystyrene spheres were assembled over glassy carbon by adding 10 μL of a 0.5 wt% aqueous suspension containing 1.0×10^{-6} mol L^{-1} Triton X-100. After slow evaporation of water, another 10 μL aliquot of the suspension was deposited over the previously layer and the water was slowly evaporated again. After that, the electrodes were placed in an oven at 100 °C for 4 h.

For CuHCNFe/Ppy deposition, the $Fe(CN)_6^{3-}$ ions were initially incorporated in the polymer matrix by potential cycling a glassy carbon electrode in a solution containing 2.0×10^{-2} mol L^{-1} $K_3Fe(CN)_6$ + 1.5×10^{-2} mol L^{-1} pyrrole + 1.0×10^{-1} mol L^{-1} KCl. The electrode was cycled in a range of −0.25 to +0.95 V at 50 mV s^{-1}. The electrodeposition was started only after 30 min, in order to swell the interspaces among polystyrene particles by the deposition solution The second step consisted of placing the $Fe(CN)_6^{3-}$/Ppy modified electrode in a solution containing 2.0×10^{-2} mol L^{-1} $CuCl_2$ + 1.0×10^{-1} mol L^{-1} KCl for 2 h. This procedure was carried out to allow the insertion of Cu^{2+} ions into the $Fe(CN)_6^{3-}$-doped polypyrrole network. After this time, the electrode was cycled in a potential range of −0.25 to +0.95 V at 50 mV s^{-1}. The polystyrene template was dissolved by soaking the electrode in stirred toluene for 24 h. After that, the modified electrode was washed and dried in a desiccator.

2.4. Synthesis of Prussian blue and CuHCNFe into mesoporous TiO_2 films

ITO electrodes (indium-tin oxide, one side coated glass by Delta Technologies Ltd., Rs <25 Ω) were used to deposit mesoporous TiO_2 films as described elsewhere [19,20]. This procedure allowed the synthesis of TiO_2 films with porous channels of 13 nm in diameter and thicknesses of 130, 200 and 260 nm. Not only thickness, but also the pore diameter could be modulated by changing the experimental procedure as described previously [17]. In this case, polypropyleneglycol and tetrahydrofuran were used to produce two new mesoporous TiO_2 platforms, one formed by channels with 20 nm diameter and another formed by channels of 40 nm in diameter.

The immobilization of Prussian blue inside mesoporous TiO_2 films was performed using the methodology described previously [18]. Briefly, the bifunctional ligand 1,10-phenantroline-5,6-dione was bind to the Ti(IV) surface by immersing the TiO_2 platforms in a 5.0×10^{-1} mol L^{-1} ethanolic solution of the ligand for 24 h. After that, the nitrogen atoms on the ligand remained available for coordination. Thus, the substrate was immersed in a 5.0×10^{-1} mol L^{-1} $FeSO_4$ solution, where Fe^{2+} cation coordination was performed. Subsequent exposure of this modified electrode to a 5.0×10^{-1} mol L^{-1} $K_3Fe(CN)_6$ solution led to the formation of one layer of Prussian blue. The immersion sequence in Fe^{2+} and $Fe(CN)_6^{3-}$ solutions could be then repeated in order to grow a new Prussian blue layer over the previously deposited.

This procedure was also adapted for CuHCNFe formation on the surface of mesoporous TiO_2 films. After immobilising the 1,10-phenanthroline-5,6-dione ligand, the electrode was immersed in an aqueous solution containing 5.0×10^{-1} mol L^{-1} $CuCl_2$ for 30 min and washed with deionised water. After, the electrode was immersed for 30 min in a 5.0×10^{-1} mol L^{-1} aqueous solution of $K_3Fe(CN)_6$ and washed once more with deionised water. Repetition of the dipping process in $CuCl_2$ and $K_3Fe(CN)_6$ solutions was capable of forming another CuHCNFe monolayer on top of the previous one.

2.5. Electrochemical detection of H_2O_2

H_2O_2 electrochemical detection was performed with macroporous and mesoporous electrocatalysts by chronoamperometry. A solution containing 5 mL of 1.0×10^{-1} mol L^{-1} NaCl (or KCl – see caption of the figures) + 1.0×10^{-1} mol L^{-1} HCl was used with slight magnetic stirring. Initially, the electrodes were polarized to 0.00 V for 40 min to stabilize the background current.

3. Results and discussion

The FESEM images obtained after removing the template of polystyrene spherical particles are presented from Fig. 1A–D. All of the macroporous films were electrodeposited controlling the charge during synthesis, so that the electrodes were always modified with similar amounts of material. These films were electrochemically characterized in media containing only cations able to block Prussian blue electroactivity, such as Na^+ and H^+. As shown in Fig. S1 (ESI), it was possible to observe the reversible oxidation and reduction of the hybrid compound at different scan rates.

The analytical performance on H_2O_2 detection of non-porous CuHCNFe/Ppy electrodes was compared with the results obtained with macroporous films presenting 300, 460, 600 and 800 nm in

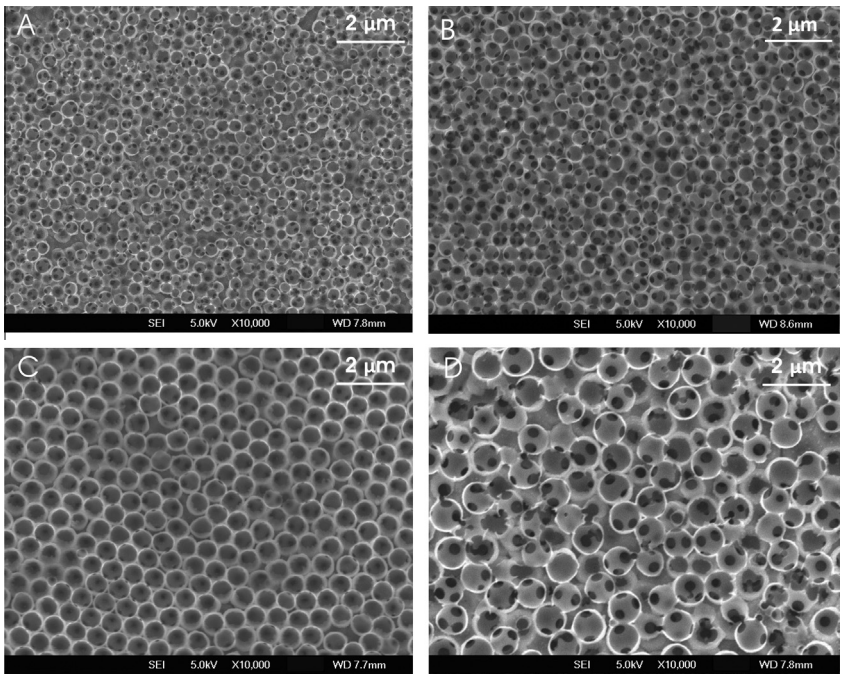

Fig. 1. FESEM images of CuHCNFe/Ppy films synthesised around polystyrene spheres with diameters of (A) 300, (B) 460, (C) 600 and (D) 800 nm.

diameter. The obtained chronoamperograms are shown in Fig. S2 (ESI). The analytical parameters obtained using the curves are presented in Table 1. The detection limits are three times the standard deviation of the background current without analyte/sensitivity, and the response time was 90% of total current variation when H_2O_2 aliquots were added.

Surprisingly, there was not considerable variation in the performance of the macroporous electrocatalysts and, moreover, no difference was observed when the results were compared with the performance of the non-porous CuHCNFe/Ppy material. An explanation for these results required to determine whether detection of H_2O_2 by CuHCNFe/Ppy was a surface phenomenon or it was dependent on the amount of material present in the electrode. If the film was very permeable to H_2O_2, detection could occur throughout the electrocatalyst volume. Consequently, all the sensors could present the same performances because all the electrodes were modified with the same amount of electrocatalyst. Table S1 (ESI) presents the measured sensitivities for four films with different amounts of non-porous CuHCNFe/Ppy that were used for H_2O_2 detection showing that the obtained sensitivities were very similar, regardless of the different charges observed during voltammetric deposition of non-porous CuHCNFe/Ppy. This result suggests that the reduction of H_2O_2 by CuHCNFe/Ppy does not depend on the volume of material but occurs mainly in the outer surface of the electrocatalyst.

Consequently, the determination of how much the surface is increased by using macroporous CuHCNFe/Ppy films becomes another important aspect for understanding the presented analytical results. With this purpose, the thicknesses of all macroporous electrocatalysts were determined by FESEM, as illustrated in Fig. S3 (ESI) and the results are summarized in Fig. 2.

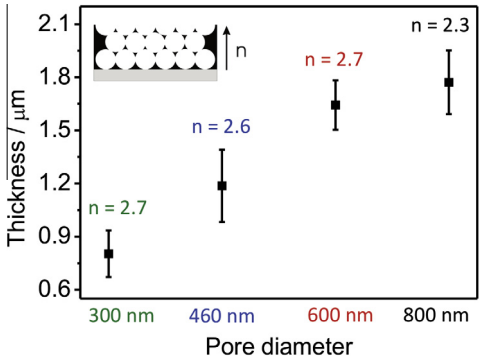

Fig. 2. Thickness obtained using the methodology presented in Fig. S3 for CuHCNFe/Ppy synthesised around spheres of 300, 460, 600 and 800 nm of diameter. The graph also shows the "*n*" values obtained for each pore size, where *n* = the average thickness (nm)/diameter of the sphere used as template (nm).

It can be observed that CuHCNFe/Ppy electrocatalysts with larger pores were thicker than those synthesised around polystyrene spheres with smaller diameters. However, dividing the average thickness by the diameter of the sphere used as a template, it was possible to estimate that all macroporous CuHCNFe/Ppy were formed by approximately 2.5 porous layers. When a macroporous film of CuHCNFe/Ppy is compared with non-porous CuHCNFe/Ppy material, the theoretical value of the increase in surface area can

Table 1
Analytical parameters obtained using CuHCNFe/Ppy with different sizes of macropores and a non-nanostructured electrocatalyst. Number of samples considered for statistics = 3.

	Non-nanostructured	300 nm	460 nm	600 nm	800 nm
Sensitivity ($\mu A\ cm^{-2}\ mmol^{-1}\ L$)	(198 ± 6)	(180 ± 20)	(190 ± 30)	(200 ± 20)	(170 ± 30)
Detection limit ($\mu mol\ L^{-1}$)	(1.9 ± 0.1)	(3 ± 1)	(3 ± 2)	(1.0 ± 0.3)	(2 ± 1)
Linear range ($mmol\ L^{-1}$)	(4.0 ± 0.2)	(3.2 ± 0.2)	(3.0 ± 0.5)	(2.2 ± 0.2)	(2.2 ± 0.2)
Response time (s)	(3.5 ± 0.7)	(3 ± 1)	(4 ± 1)	(5 ± 2)	(5 ± 3)

be estimated on the basis of geometric considerations, leading to Eq. (1), where "*f*" is the factor of increase in surface area when compared with a "flat" deposit, and "*n*" is the number of porous layers [21,22].

$$f = n\pi\left(\sqrt{\frac{4}{3}}\right) \quad (1)$$

For $n = 2.5$, the factor of increased surface area corresponds to $f = 9$, which means that all macroporous CuHCNFe/PPy films have a theoretical surface area approximately nine times greater than the non-porous CuHCNFe/Ppy. This might help to understand why the performance of all macroporous CuHCNFe/PPy are similar to each other but does not explain why there is no advantage in using these macrostructures instead of the non-porous material. Because of that, the wettabilities of the macroporous and non-porous CuHCNFe/Ppy electrocatalysts were studied through contact angle measurements, with the purpose of understanding how difficult was the pore accessibility by the aqueous solutions where H_2O_2 tests were performed. [23–25]. Fig. S4 (ESI) shows the images obtained when a drop of an aqueous solution containing 1.0×10^{-1} mol L^{-1} NaCl + 1.0×10^{-1} mol L^{-1} HCl was placed on macroporous and non-porous CuHCNFe/Ppy electrocatalysts. Fig. 3 displays the measured contact angles for the different platforms.

As shown in Fig. 3, there is no significant difference between the contact angles of any of the macroporous CuHCNFe/PPy, which were above 90° in all the cases, indicating a hydrophobic surface. These angles were greater than that of non-porous CuHCNFe/Ppy, which was approximately (65 ± 4)°. This difference is attributable to the air trapped within the pores, which indicates that the present porous system follows the behavior of the model proposed by Cassie and Baxter [23]. This phenomenon makes the access to the inner active sites of the macroporous CuHCNFe/PPy by the electrolyte solution, more difficult. We therefore added the surfactant sodium dodecyl sulfate (SDS) to the 0.1 mol L^{-1} NaCl + 0.1 mol L^{-1} HCl solution to alter the surface tension and improve wettability of the macroporous electrocatalyst, causing complete filling of the pores [26]. Fig. S5 (ESI) presents the contact angle measurements carried out on macroporous CuHCNFe/Ppy-460 nm; the use of various concentrations of surfactant allowed an effective transition from a Cassie-Baxter to a Wenzel system. Experiments for H_2O_2 detection were repeated with CuHCNFe/Ppy-460 nm, in the presence of SDS surfactant. The experiments were performed with electrolyte solutions containing 1.0×10^{-1}, 1.0×10^{-2} and 1.0×10^{-4} mol L^{-1} surfactant, to verify whether the number of amphiphilic molecules in the environment could alter the results. The obtained sensitivities are shown in Fig. S6 (ESI); the performances were again quite similar among all of the considered systems, suggesting that even with complete accessibility of the pores there is another factor affecting the results. This factor is related to kinetics and, as already demonstrated by Szamocki et al. [27], it plays a key role in the use of macroporous platforms for electrochemical sensors. For fast electrochemical kinetics, molecules react completely in the pores of the outer half layer before reaching the innermost pores. Once CuHCNFe/Ppy is an electrocatalyst poorly permeable to H_2O_2 reduction, only a small part of the outer macroporous CuHCNFe/Ppy area is used for the reaction, and as a result, the current is always constant. Alternatively, electrochemical reactions with slow kinetics allow the utilization of all porous layers.

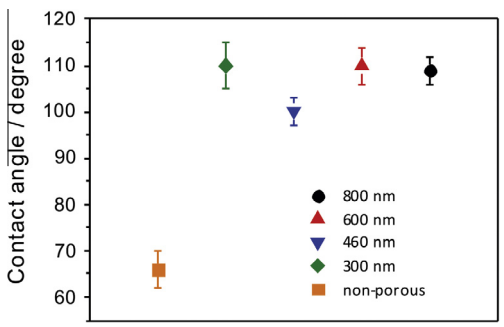

Fig. 3. The contact angle between the tangent of the liquid–vapor interface and the tangent of the liquid–solid interface. Number of angles measured for each pore size = 6.

These results are interesting because they show that efforts performed to increase surface area of porous electrodes do not always bring advantages to analytical performance of sensors. Consequently, to interpret the analytical application of porous films, it is important to answer the following questions: Does the sensor response depend on surface area or volume of the material? Can the inner pores be accessible by the analyte? Does the kinetic allow the utilization of inner pores or the reaction is so fast that occurs only at outer half pores?

We were also interested to observe how these questions were manifested in electrodes modified by Prussian blue type electrocatalystys with smaller pores, when the macroscale is diminished to the nanoscale. As shown recently [18], mesoporous TiO_2 thin films presenting pore arrays with 13 nm in diameter and a thickness of 130 nm were functionalized with a bifunctional ligand (1,10-phenantroline-5,6-dione) that allowed the immobilization of Fe^{2+} ions with open coordination sites on the mesoporous surface. The system was exposed to a $Fe(CN)_6^{3-}$ solution to assemble a monolayer of Prussian blue inside the mesoporous matrix. Alternating immersions in Fe^{2+} and $Fe(CN)_6^{3-}$ solutions were repeated to add more Prussian blue layers to the mesoporous material, and the results achieved during H_2O_2 detection showed that the sensitivity of the sensor increased to up to 4 confined layers, presenting a good chronoamperometric result of (410 ± 20) μA cm^{-2} $mmol^{-1}$ L.

Different from CuHCNFe/Ppy, it is well known that Prussian blue alone presents a good permeability to H_2O_2, once there is no polypyrrole diminishing the hydrophilic character of the system [28,29]. So, experiments were carried out to study the way in which kinetics could affect the performance of the sensor. Because of that, mesoporous TiO_2 electrodes formed by pore arrays with an average diameter of 13 nm were prepared with thickness of 130, 200 and 260 nm. These platforms were modified with 4 layers of Prussian blue and the results achieved for H_2O_2 detection using the films with different thickness are shown in Fig. S7 (ESI). The obtained sensitivities were similar and independent on the thickness of the employed mesoporous materials. It is noteworthy that, as in the case of macroporous CuHCNFe/Ppy, Prussian blue is also a catalyst for H_2O_2 electroreduction. Consequently, the fast kinetics of the reaction turns only the outer Prussian blue active sites responsible for reducing H_2O_2, even though the mesoporous material presents nanometer-scale film thickness while the macroporous CuHCNFe/Ppy thickness is on the micrometer scale.

In another set of experiments, the thickness was maintained at 130 nm and the pore size of mesoporous TiO_2 films was changed. Platforms with 13, 20 and 40 nm in diameter were used to immobilize Prussian blue layers into their cavities. Then, electrodes were applied for H_2O_2 detection in 1.0×10^{-1} mol L^{-1} KCl + 1.0×10^{-1} mol L^{-1} HCl. The obtained sensitivities for each pore size in function of the number of immobilized Prussian blue layers are shown in Fig. 4.

Fig. 4 shows that when thickness was maintained at 130 nm, for each pore size, the sensitivities were dependent on the material volume and they increased until a specific number of immobilized layers before declining substantially. We have shown for the platform with 13 nm in diameter [18] that the values of the

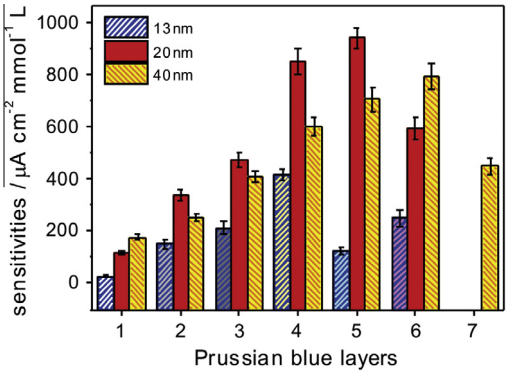

Fig. 4. Sensitivities obtained during H_2O_2 detection with mesoporous TiO_2 electrodes formed by pore arrays with diameters of 13, 20 or 40 nm and thickness of 130 nm. During experiments, aliquots of 5 μL of 1.0×10^{-1} mol L^{-1} H_2O_2 were added to 5 mL of a solution of 1.0×10^{-1} mol L^{-1} KCl + 1.0×10^{-1} mol L^{-1} HCl. E = 0.00 V vs $Ag/AgCl/KCl_{sat}$.

sensitivities and their relation with the number of Prussian blue layers can be explained using UV–Vis spectroscopy and scanning electron microscopy data. When a few layers of Prussian blue were confined into the pores with 13 nm, FESEM images revealed that the pores remained open and accessible to H_2O_2, while UV–Vis data revealed a blue-shifted metal-to-metal charge transition, indicating an unusual and more reactive Prussian blue structure. Furthermore, the sensitivity increased until the immobilization of 4 layers because it was possible to confine the greatest amount of Prussian blue electrocatalyst inside the pores of 13 nm without blocking the cavities. Finally, the immobilization of the 5th Prussian blue layer made the sensitivity to decline because the pores were completely filled, leading to the loss of nanoporous morphology, as represented in Fig. S8A (ESI). The UV–Vis data obtained with electrocatalysts where pores were blocked also revealed that the metal-to-metal charge transition was very similar to that observed with a non-porous Prussian blue material, indicating that coordination of a large amount of layers diminishes the number of defects present in the material, as depicted in Fig. S8B (ESI).

This explanation can also be applied to the new platforms with 20 and 40 nm in diameter. However, note that the number of Prussian blue layers that can be immobilized before diminishing the sensitivity varied as a function of the pore diameter. For pores of 13 nm, it was possible to confine accessible and reactive active sites up to 4 layers, and the sensitivity reached (410 ± 20) μA cm^{-2} $mmol^{-1}$ L. For pores of 20 nm, the sensitivity increased until immobilizing 5 layers, where it reached a value of (940 ± 40) μA cm^{-2} $mmol^{-1}$ L. The possibility of increasing the number of deposited layers before losing the confinement effect was attributed to the fact that the platforms of 20 nm in diameter present pores with greater diameters than the systems with pores of 13 nm. This result becomes even more interesting when we observe the sensitivity of the films immobilized into the platforms with 40 nm in diameter, which increased until the 6th layer, before decreasing because the pores were completely obstructed. However, even with larger pores, the sensitivity obtained immobilizing 6 layers of Prussian blue into the pores of 40 nm was (790 ± 50) μA cm^{-2} $mmol^{-1}$ L, lower than that displayed by confining 5 Prussian blue layers into the pores of 20 nm. This original result indicates that the gain in accessibility achieved with the pores of 40 nm does not improve the analytical performance of the sensor during H_2O_2 detection when compared to the sensor prepared with pores of 20 nm. Consequently, it is necessary to consider a compromise between the amount of immobilized electrocatalyst and the accessibility of H_2O_2 in order to understand the analytical performance of the present mesoporous Prussian blue sensors.

Finally, many reports have shown that the activity of Prussian blue can be blocked in the presence of Na^+, H^+, Li^+ and the group II cations [30,31] depending on the conditions in which Prussian blue was deposited. An alternative to this limitation replaces Prussian blue with an analogue with larger vacancies in its inorganic structure, such as CuHCNFe. Maintaining the same strategy of electrocatalyst immobilization, sequential immersions in Cu^{2+} and $Fe(CN)_6^{3-}$ solutions could be performed to control the number of CuHCNFe layers present in the TiO_2 mesostructure. Using this methodology, TiO_2 platforms with pore sizes of 13, 20 and 40 nm in diameter were used to confine 4, 5 and 6 layers of CuHCNFe, respectively. Fig. S9 (ESI) presents the sensitivities obtained when these electrocatalysts were applied to detect H_2O_2 in an electrolyte containing Prussian blue blocking cations. For comparative purposes, the graph also includes the sensitivities obtained in the same electrolyte using TiO_2 platforms with pore sizes of 13, 20 and 40 nm in diameter modified with 4, 5 and 6 layers of Prussian blue, respectively. The analytical curves achieved by confining 5 layers of CuHCNFe or Prussian blue into TiO_2 with pore sizes of 20 nm are presented in Fig. 5, in comparison with the result achieved with a conventionally non-porous Prussian blue material.

From Figs. S9 (ESI) and 5, it is possible to see that the sensitivities achieved with the nanoporous platforms modified with CuHCNFe (332 μA cm^{-2} $mmol^{-1}$ L for pores of 13 nm, 637 μA cm^{-2} $mmol^{-1}$ L for pores of 20 nm and 560 μA cm^{-2} $mmol^{-1}$ L for pores of 40 nm) in media containing Na^+ and H^+ were extremely high, especially when compared to previously reported sensitivities. For example, a non-porous CuHCNFe film presents a sensitivity of 0.14 μA cm^{-2} $mmol^{-1}$ L [16], while systems with CuHCNFe nanoparticles shows sensitivities of 30.6 μA cm^{-2} $mmol^{-1}$ L [32]. In spite of these results, an even more striking performance was obtained with the Prussian blue modified sensors in media containing Na^+ and H^+. Just as in media with K^+ ions, films with pores of 20 nm showed a better performance than pore sizes of 13 or 40 nm, reaching a sensitivity of (930 ± 50) μA cm^{-2} $mmol^{-1}$ L. To the best of our knowledge, this result is extremely satisfactory considering chronoamperometric experiments performed in medium containing Prussian blue blocking cations. Moreover, mesoporous Prussian blue also showed an improved performance when compared to the conventional electrodeposited Prussian blue, which sensitivity obtained in Na^+ was only 82 μA cm^{-2} $mmol^{-1}$ L and the linear range did not exceed 0.15 mmol L^{-1} (one order of magnitude lower than that exhibited by mesoporous Prussian blue sensor). The limit of detection

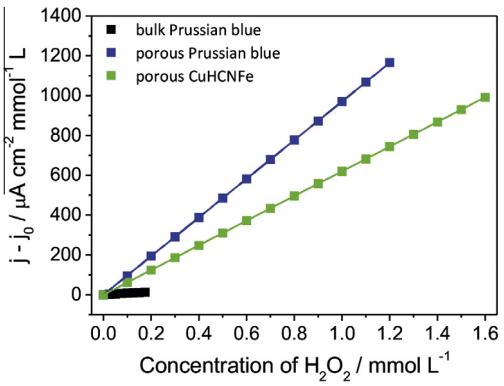

Fig. 5. Analytical curves obtained by confining 5 layers of CuHCNFe or Prussian blue into TiO_2 films with pore sizes of 20 nm, in comparison with the result achieved with a conventionally non-porous Prussian blue material. During experiments, aliquots of 5 μL of 1.0×10^{-1} mol L^{-1} H_2O_2 were added to 5 mL of a solution of 1.0×10^{-1} mol L^{-1} NaCl + 1.0×10^{-1} mol L^{-1} HCl. For non-porous Prussian blue, aliquots of 5 μL of 2.0×10^{-2} mol L^{-1} H_2O_2 were added to the electrolyte. E = 0.00 V vs $Ag/AgCl/KCl_{sat}$.

obtained with the mesoporous Prussian blue was (0.49 ± 0.08) μmol L^{-1} (3 times the standard deviation of the background current without analyte/sensitivity), the response time was (6 ± 2) (90% of the current variation) and the linear range was up to (1.3 ± 0.1) mmol L^{-1}.

The results achieved here suggest that Prussian blue immobilised by coordination in the TiO_2 platforms with pores of 13, 20 or 40 nm presents an inorganic structure different from the displayed by the non-porous electrocatalyst. The spectra in the visible region shown in Fig. S8B (ESI) supports this hypothesis because the electronic transition of the mesoporous electrocatalyst was shifted to shorter wavelengths when compared to that currently exhibited by Prussian blue. This different structure contributes to the high reactivity of the material and allows insertion/removal of Na^+ during charge compensation without losing electroactivity. It is important to emphasize that all porous Prussian blue materials were synthesised with the same experimental conditions, once incorporation of different M^{z+} cations during charge neutralization could also affect the energy of the charge-transfer band [33]. Moreover, as shown in Fig. S10 (ESI), the better wettability of this material also favors electrochemical experiments performed in aqueous solution. The low contact angle of (33 ± 2)° (number of angles measured = 4) indicates that this platform is hydrophilic, unlike the hydrophobic macroporous CuHCNFe/Ppy reported in Fig. 3, with contact angles above 90°. This difference in the contact angle measurements of the porous electrocatalysts can be explained as a function of the different physical–chemical natures of the materials and due to the greater amount of air trapped in the macroporous system.

For comparison, to the best of our knowledge, the highest sensitivity achieved with a Prussian blue based sensor was reported recently by Karyakin and col. [34], where a macroporous gold microelectrode was utilized for Prussian blue electrodeposition. The sensitivity obtained for H_2O_2 sensing was 8.8 ± 0.7 A mol L^{-1} - cm^{-2} in a batch regime under stirring at 0.00 V; in a 0.05 mol L^{-1} phosphate buffer solution, pH 7.0, and containing KCl 0.1 mol L^{-1}. Interestingly, when the pores of the microelectrode surface were completely filled with the electrocatalyst, the resulting sensor also showed a behavior similar to the non-porous microelectrode.

4. Conclusions

Efforts performed to increase surface area of porous electrodes do not always bring advantages to analytical performance of electrochemical sensors. In order to evaluate the situations where their use is recommended, important questions must be answered: does the sensor response depend on surface area or volume of the material? Can the inner pores be accessible by the analyte? Does the kinetic allow the utilization of inner pores or the reaction is so fast that occurs only at outer half pores?

Macroporous CuHCNFe/Ppy sensors with diameters from 300 to 800 nm, in spite of increasing the surface area/volume ratio when compared to the non-porous analogue, presented analytical results that indicate that kinetics involved in the electrochemical reaction made it occur only in the outer pores of the material. Once CuHCNFe/Ppy presented poor permeability to H_2O_2, the electrochemical responses were independent of the macropore size. Oppositely, porous Prussian blue based sensors prepared at nanoscale presented the ability to modulate the performance according to the size of the pore and number of immobilized layers. By changing these parameters, it was possible to observe the influence of the confinement effect on reactivity. Kinetic parameters also played an important role on mesoporous platforms, once it was shown that only the external active sites of the mesoporous Prussian blue were participating in H_2O_2 detection. However, the good permeability of the material to H_2O_2 created a compromise between accessibility and the amount of external immobilized layers of electrocatalyst, which allowed the achievement of a mesoporous Prussian blue sensor presenting a sensitivity of sensitivity of (930 ± 50) μA cm^{-2} $mmol^{-1}$ L, detection limit of (0.49 ± 0.08) μmol L^{-1}, response time of (6 ± 2) seconds and linear range up to (1.3 ± 0.1) mmol L^{-1}. This performance is extremely satisfactory considering sensors operating by chronoamperometry in Prussian blue blocking cations.

Acknowledgments

The authors are thankful to INCT Bioanalítica, FAPESP (09/53199-3), CNPq, UBACyT, ANPCyT (PICT 2004-25409 and 2005-34518). A.O.P.B. and V.R.G. thank FAPESP (proc. 10/08245-4, 05/59560-9 and 11/15159-0) for the scholarships received. The authors also thank Prof. Dr. Denise F.S. Petri for contact angle measurements.

Appendix A. Supplementary material

Supplementary data associated with this article can be found, in the online version, at http://dx.doi.org/10.1016/j.jelechem.2013.07.029.

References

[1] A. Walcarius, A. Kuhn, Ordered porous thin films in electrochemical analysis, Trends Anal. Chem. 27 (2008) 593–603.
[2] V.R. Gonçales, R.P. Salvador, M.R. Alcântara, S.I. Córdoba de Torresi, On the template synthesis of nanostructured inorganic/organic hybrid films, J. Electrochem. Soc. 155 (2008) K140–145.
[3] V.R. Gonçales, M.P. Massafera, T.M. Benedetti, D.G. Moore, S.I. Córdoba de Torresi, R.M. Torresi, Nanostructured thin films obtained by electrodeposition over a colloidal crystal template: applications in electrochemical devices, J. Braz. Chem. Soc. 20 (2009) 663–673.
[4] J.-D. Qiu, H.-Z. Peng, R.-P. Liang, M. Xiong, Preparation of three-dimensional ordered macroporous Prussian blue film electrode for glucose biosensor application, Electroanal. 19 (2007) 1201–1206.
[5] P.N. Bartlett, S. Guerin, A micromachined calorimetric gas sensor: an application of electrodeposited nanostructured palladium for the detection of combustible gases, Anal. Chem. 75 (2003) 126–132.
[6] A.A. Karyakin, E.A. Puganova, I.A. Budashov, I.N. Kurochkin, E.E. Karyakina, V.A. Levchenko, V.N. Matveyenko, S.D. Varfolomeyev, Prussian Blue based nanoelectrode arrays for H_2O_2 detection, Anal. Chem. 76 (2004) 474–478.
[7] E.A. Puganova, A.A. Karyakin, New materials based on nanostructured Prussian blue for development of hydrogen peroxide sensors, Sens. Actuators B-Chem. 109 (2005) 167–170.
[8] P.N. Bartlett, J.J. Baumberg, P.R. Birkin, M.A. Ghanem, M.C. Netti, Highly ordered macroporous gold and platinum films formed by electrochemical deposition through templates assembled from submicron diameter monodisperse polystyrene spheres, Chem. Mater. 14 (2002) 2199–2208.
[9] T. Sumida, Y. Wada, T. Kitamura, S. Yanagida, Electrochemical preparation of macroporous polypyrrole films with regular arrays of interconnected spherical voids, Chem. Commun. 17 (2000) 1613–1614.
[10] G.S. Attard, P.N. Bartlett, N.R.B. Coleman, J.M. Elliott, J.R. Owen, J.H. Wang, Mesoporous platinum films from lyotropic liquid crystalline phases, Science 278 (1997) 838–840.
[11] A.A. Karyakin, E.A. Kuritsyna, E.E. Karyakina, V.L. Sukhanov, Diffusion controlled analytical performances of hydrogen peroxide sensors: towards the sensor with the largest dynamic range, Electrochim. Acta 54 (2009) 5048–5052.
[12] D. Lowinsohn, M. Bertotti, Flow injection analysis of blood L-lactate by using a Prussian Blue-based biosensor as amperometric detector, Anal. Biochem. 365 (2007) 260–265.
[13] P.A. Fiorito, V.R. Gonçales, E.A. Ponzio, S.I. Córdoba de Torresi, Synthesis, characterization and immobilization of Prussian blue nanoparticles. A potential tool for biosensing devices, Chem. Commun. 3 (2005) 366–368.
[14] I. Luiz de Mattos, L. Gorton, T. Laurell, A. Malinauskas, A.A. Karyakin, Development of biosensors based on hexacyanoferrates, Talanta 52 (2000) 791–799.
[15] P.A. Fiorito, S.I. Córdoba de Torresi, Hybrid nickel hexacyanoferrate/polypyrrole composite as mediator for hydrogen peroxide detection and its application in oxidase-based biosensors, J. Electroanal. Chem. 581 (2005) 31–37.
[16] P.A. Fiorito, C.M.A. Brett, S.I. Córdoba de Torresi, Polypyrrole/copper hexacyanoferrate hybrid as redox mediator for glucose biosensors, Talanta 69 (2006) 403–408.

[17] L. Malfatti, M.G. Bellino, P. Innocenzi, G.J.A.A. Soler-Illia, One-pot route to produce hierarchically porous titania thin films by controlled self-assembly, swelling, and phase separation, Chem. Mater. 21 (2009) 2763–2769.
[18] M. Gaitán, V.R. Gonçales, G.J.A.A. Soler-Illia, L.M. Baraldo, S.I. Córdoba de Torresi, Structure effects of self-assembled Prussian blue confined in highly organized mesoporous TiO_2 on the electrocatalytic properties towards H_2O_2 detection, Biosens. Bioelectron. 26 (2010) 890–893.
[19] E.L. Crepaldi, G.J.A.A. Soler-Illia, D. Grosso, C. Sanchez, Nanocrystallised titania and zirconia mesoporous thin films exhibiting enhanced thermal stability, New J. Chem. 27 (2003) 9–13.
[20] E.L. Crepaldi, G.J.A.A. Soler-Illia, D. Grosso, F. Cagnol, F. Ribot, C. Sanchez, Controlled formation of highly organized mesoporous titania thin films: From mesostructured hybrids to mesoporous nanoanatase TiO_2, J. Am. Chem. Soc. 125 (2003) 9770–9786.
[21] R. Szamocki, A. Velichko, F. Muucklich, S. Reculusa, S. Ravaine, S. Neugebauer, W. Schuhmann, R. Hempelmann, A. Kuhn, Improved enzyme immobilization for enhanced bioelectrocatalytic activity of porous electrode, Electrochem. Commun. 9 (2007) 2121–2127.
[22] R. Szamocki, A. Velichko, C. Holzapfel, F. Muucklich, S. Ravaine, P. Garrigue, N. Sojic, R. Hempelmann, A. Kuhn, Macroporous ultramicroelectrodes for improved electroanalytical measurements, Anal. Chem. 79 (2007) 533–539.
[23] A. Marmur, Soft contact: measurement and interpretation of contact angles, Soft Matter 2 (2006) 12–17.
[24] M.E. Abdelsalam, P.N. Bartlett, T. Kelf, J. Baumberg, Wetting of regularly structured gold surfaces, Langmuir 21 (2005) 1753–1757.
[25] A. Checco, T. Hofmann, E. DiMasi, C.T. Black, B.M. Ocko, Morphology of air nanobubbles trapped at hydrophobic nanopatterned surfaces, Nano Lett. 10 (2010) 1354–1358.
[26] M.A. Ghanem, P.N. Bartlett, P. de Groot, A. Zhukov, A double templated electrodeposition method for the fabrication of arrays of metal nanodots, Electrochem. Commun. 6 (2004) 447–453.
[27] R. Szamocki, S. Reculusa, S. Ravaine, P.N. Bartlett, A. Kuhn, R. Hempelmann, Tailored mesostructuring and biofunctionalization of gold for increased electroactivity, Angew. Chem. Int. Ed. 45 (2006) 1317–1321.
[28] A.V. Borisova, E.E. Karyakina, S. Cosnier, A.A. Karyakin, Current-free deposition of Prussian blue with organic polymers: towards improved stability and mass production of the advanced hydrogen peroxide transducer, Electroanal. 21 (2009) 409–414.
[29] A.A. Karyakin, E.E. Karyakina, L. Gorton, The electrocatalytic activity of Prussian blue in hydrogen peroxide reduction studied using a wall-jet electrode with continuous flow, J. Electroanal. Chem. 456 (1998) 97–104.
[30] F. Ricci, G. Palleschi, Sensor and biosensor preparation, optimisation and applications of Prussian Blue modified electrode, Biosens. Bioelectron. 21 (2005) 389–407.
[31] K. Itaya, I. Uchida, V.D. Neff, Electrochemistry of polynuclear transition-metal cyanides - Prussian blue and its analogues, Acc. Chem. Res. 19 (1986) 162–168.
[32] A.P. Baioni, M. Vidotti, P.A. Fiorito, S.I. Córdoba de Torresi, Copper hexacyanoferrate nanoparticles modified electrodes: A versatile tool for biosensors, J. Electroanal. Chem. 622 (2008) 219–224.
[33] D.R. Rosseinsky, H. Lim, H. Jiang, J. Wei Chai, Optical charge-transfer in iron(III)hexacyanoferrate(II): electro-intercalated cations induce lattice-energy-dependent ground-state energies, Inorg. Chem. 42 (2003) 6015–6023.
[34] A.V. Mokrushina, M. Heim, E.E. Karyakina, A. Kuhn, A.A. Karyakin, Enhanced hydrogen peroxide sensing based on Prussian Blue modified macroporous microelectrodes, Electrochem. Commun. 29 (2013) 78–80.